Single Wall Carbon Nanotube/Polyethylene Nanocomposites: Thermal and Electrical Conductivity

Reto Haggenmueller,† Csaba Guthy,† Jennifer R. Lukes,‡ John E. Fischer,† and Karen I. Winey*,†

Department of Materials Science and Engineering and Department of Mechanical Engineering & Applied Mechanics, University of Pennsylvania, Philadelphia, Pennsylvania 19104-6272

Received July 5, 2006; Revised Manuscript Received January 31, 2007

ABSTRACT: The thermal and electrical conductivities in nanocomposites of single walled carbon nanotubes (SWNT) and polyethylene (PE) are investigated in terms of SWNT loading, the degree of PE crystallinity, and the PE alignment. Isotropic SWNT/PE nanocomposites show a significant increase in thermal conductivity with increasing SWNT loading, having 1.8 and 3.5 W/mK at a SWNT volume fraction of $\phi \sim 0.2$ in low-density PE (LDPE) and high-density PE (HDPE), respectively. This increase in SWNT/HDPE is more than additive and suggests a reduction of the interfacial thermal resistance. Fitting the thermal conductivity data of the SWNT/HDPE nanocomposites with two models indicates that the thermal conductivity relies on a percolating SWNT network. Oriented SWNT/HDPE nanocomposites exhibit higher thermal conductivities, which are attributed primarily to the aligned PE matrix.

Introduction

Carbon nanotubes are promising fillers for composite materials to improve mechanical behavior and electrical and thermal transport. Theoretical[1] and experimental work[2−4] show an uniquely high thermal conductivity of more than 3000 W/mK for multi-wall carbon nanotubes (MWNT) and single-wall carbon nanotubes (SWNT). Experiments to date report modest increases in the thermal conductivity of organic fluids or polymers when filled with relatively low volume fractions of carbon nanotubes.[5−10] Liquids and amorphous polymers generally have low thermal conductivities because they restrict the phonon mobility through the composite matrix and have large interfacial thermal resistances at the nanotube−matrix interface.[11,12]

Here we focus on a *semicrystalline* polymer, polyethylene, that shows an enhancement in thermal conductivity with increasing crystallinity.[13] Moreover, polyethylene exhibits a dramatic increase in thermal conductivity with increasing alignment of polymer chains due to the formation of long needlelike crystals in highly drawn fibers.[14] Thermal conductivities as high as 340 W/mK can be achieved in ultradrawn fibers. Similarly, orientation also has a profound influence on thermal conductivity in SWNT buckypapers, with a thermal conductivity at least 8 times higher for partially aligned SWNT as compared to randomly oriented nanotubes.[15]

Recently, we extensively described the morphology and crystallization kinetics of polyethylene (PE) in the presence of single wall carbon nanotubes (SWNT) in both isotropic and aligned composites.[16] We found that the SWNT in our PE composites exist predominately in small-diameter bundles (average length and diameter are 445 and 3 nm) at the concentrations considered here. Thermal analysis showed that the nanotubes provide nucleation sites for PE and accelerate the crystal growth rate while reducing the crystal dimensionality from spherulitic to disk-shaped. By comparing the orientations of SWNT and PE produced by various processing conditions, we found that SWNT bundles template the growth of PE crystals by imposing a growth direction perpendicular to the SWNT.

Here, we probe the electrical and thermal conductivity of these novel SWNT/PE nanocomposites by considering three factors to improve thermal conductivity: a crystalline matrix (polyethylene), crystalline alignment in the matrix, and aligned SWNT. The effect of the polyethylene crystallinity on the thermal conductivity in SWNT/polyethylene composites is studied in isotropic composites made with low-density and high-density polyethylenes. To investigate the effect of the orientation on the thermal conductivity, SWNT/HDPE composites were melt-spun into fibers to align both the SWNT filler and the polyethylene matrix.

Experimental Methods

The matrix polymers were low-density and high-density polyethylene (LDPE MW ∼ 35 000 g/mol and HDPE ∼ 50 000 g/mol, supplied by Aldrich) with PE crystallinities of 33% and 78%, respectively. SWNT for the nanocomposites were synthesized by the laser ablation method (supplied by NASA Johnson Space Center). Our SWNT purification protocol, hot-coagulation method to produce the composites, and melt fiber spinning method to make anisotropic nanocomposites are described elsewhere.[16] Composites were prepared with SWNT volume fractions of $\phi \sim 0.0056$ and 0.195 (1 and 30 wt %) in LDPE and $\phi \sim 0.006$, 0.03, 0.06, and 0.2 (1, 5, 10, and 30 wt %) in HDPE for nominally isotropic samples, prepared by recrystallizing composites in a hot press. Anisotropic samples were prepared by melt fiber spinning with SWNT volume fractions of $\phi \sim 0.006$ and 0.012 (1 and 2 wt %) in HDPE. The morphologies of nanotubes, PE, and SWNT/PE nanocomposites were previously extensively characterized in terms of nanotube dispersion, nanotube orientation, and PE crystal structure.[16]

The thermal conductivity was measured using a comparative method:[17] small (∼2 mm × 1 mm × 1 mm) samples were mounted in series between two constantan rods with known temperature-dependent thermal conductance. Differential type E thermocouple wires (diameter 0.0005 in.) were attached directly to the sample and the constantan rods to measure the temperature drops across each. A heater at one end of the first constantan rod provided a

* Corresponding author. E-mail: winey@seas.upenn.edu.
† Department of Materials Science and Engineering.
‡ Department of Mechanical Engineering & Applied Mechanics.

10.1021/ma0615046 CCC: $37.00 © 2007 American Chemical Society
Published on Web 03/06/2007

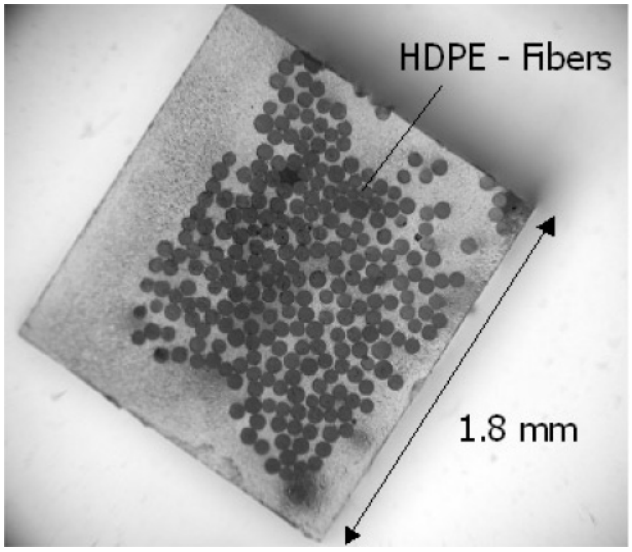

Figure 1. Cross-sectional optical micrograph of HDPE fibers embedded in epoxy to facilitate thermal conductivity measurements using the comparative method.

heat current through the rod−sample−rod series to the cold stage at the end of the second constantan rod; the thermal conductivity was calculated by comparing the temperature drops across the sample and the constantan rods. On the basis of numerous measurements of various PE standards and comparing to tabulated values, we estimate the error in thermal conductivity to be less than ±15% and arising from errors in sample dimensions and variability in the sample wiring.

For the isotropic composites, thermal conductivity specimens were simply cut from large samples. In contrast, for the anisotropic melt-spun fibers, the thermal conductance is too low for the comparative method due to their small cross-sectional area (diameters 20−100 μm). To obtain a sufficiently high conductance, approximately 200−1600 parallel fibers were embedded in epoxy (Figure 1). The thermal conductivity was measured along the fiber direction, and the fiber thermal conductivity was calculated according to the volume fraction of fiber; this volume fraction of fiber was found by determining the number of fibers, the length of the sample, and the number-average fiber diameter from cross-sectional optical microscopy. Note that the measuring error of the thermal conductivity increases to ±20% for the embedded fiber samples due to uncertainties in the nanocomposite fiber volume fraction in the epoxy.

Electrical conductivity was determined with a two-probe method for the composites and a four-probe method for pristine PE.

Results and Discussion

SWNT Loading and PE Crystallinity in Isotropic Composites. The electrical conductivities of the SWNT/LDPE and SWNT/HDPE composites exhibit typical percolation behavior at room temperature (Figure 2a). All these composites are above the percolation threshold for electrical conductivity, which is estimated as $\phi \sim 0.003$ SWNT using earlier experimental results[18,19] and model calculations based on SWNT of similar aspect ratio.[20] The fact that composites with $\phi \sim 0.006$ SWNT have electrical conductivities of $\sim 10^{-4}$ S/cm indicates that the SWNT bundles form an electrically conductive SWNT network that spans the sample. Our previous morphological study found that SWNT both nucleate and template PE crystallization,[16] such that SWNT are partially covered with PE crystallites. This formation of PE crystallites does not disrupt the electrically conductive SWNT network. Furthermore, both LDPE and HDPE composites have comparable electrical conductivities at $\phi \sim 0.006$ and 0.2, indicating comparable nanotube dispersion in both matrices.

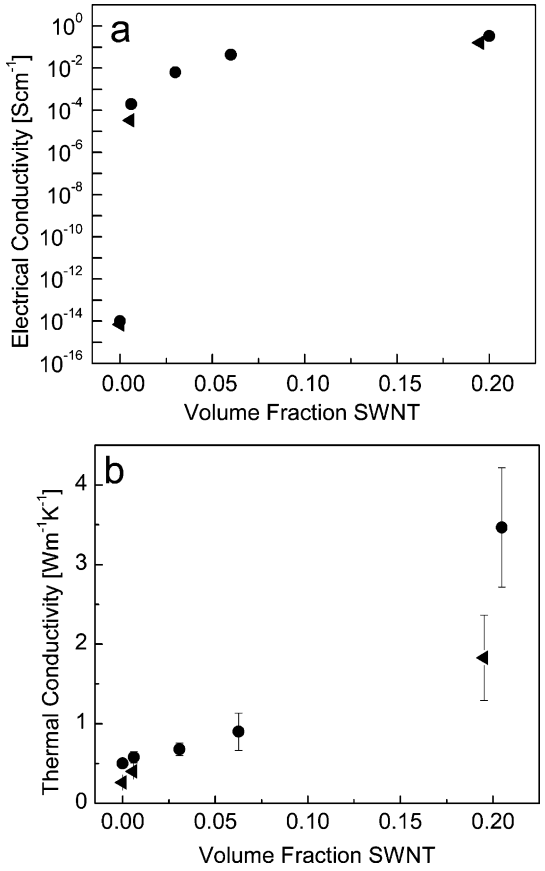

Figure 2. (a) Electrical and (b) thermal conductivity for isotropic (tilted ▲) SWNT/LDPE and (●) SWNT/HDPE composites at various SWNT loadings, measured perpendicular to pressing direction. The data points for thermal conductivity represent averages of 2−4 sample measurements with standard deviation.

The thermal conductivities of the neat LDPE (0.26 W/mK) and HDPE (0.5 W/mK) samples agree with literature values and show that higher PE crystallinity results in higher thermal conductivity in neat PE (Figure 2b). For both SWNT/LDPE and SWNT/HDPE isotropic composites the thermal conductivity moderately increases at low SWNT volume fractions ($\phi \leq 0.06$). At the highest loading, $\phi \sim 0.20$ SWNT, the LDPE composite reaches 1.8 W/mK, whereas the HDPE composite has an average thermal conductivity of 3.5 W/mK, an increase of 700% relative to neat HDPE. The behavior of the thermal conductivity in isotropic samples is notably different from the electrical conductivity.[9,21] The absence of a significant increase in thermal conductivity at low loadings is attributed to the modest difference of the constituent thermal conductivities and the large interfacial thermal resistance between the polymer matrix and SWNT, as previously described.[11,22] Weak thermal coupling between the SWNT and polymers causes large interfacial thermal resistance.

At the high SWNT loading ($\phi \sim 0.2$) the difference in thermal conductivity for LDPE and HDPE composites is significantly larger than the thermal conductivity in neat PE (1.7 and 0.24 W/mK, respectively), which implies that the contributions from the matrix and the SWNT network are not simply additive based on filler loading. The observed increase could be the result of changes at the interface between PE and SWNT. By way of contrast, graphite/LDPE and graphite/HDPE composites exhibit a straightforward increase in thermal conductive where the difference in the two types of composites is approximately constant in increasing filler loading.[23] This study of graphite/PE composites calculates the contributions to the thermal

conductivity from the amorphous and crystalline phases to be 0.091 and 0.593 W/mK, respectively. In our study, the percent crystallinity of LDPE and HDPE does not significantly change with the addition of SWNT, so the thermal conductivity of the matrix is constant with loading. Furthermore, we dismiss the possibility of significant differences in the SWNT network because both our earlier morphological study of these composites[16] and the electrical conductivity (Figure 2a) indicate no significant differences. Thus, we hypothesize that the HDPE matrix reduces the interfacial thermal resistance relative to the LDPE matrix. We have previously found that PE nucleates on SWNT in the melt state, thereby locally increasing the PE crystallinity at the SWNT/polymer interface.[16] Thus, in a HDPE matrix, PE crystallites are more likely to span between SWNT bundles at higher SWNT loadings. Bridging lamellae between SWNT could reduce the interfacial thermal resistance and consequently improve the thermal conductivity of the SWNT network in HDPE relative to LDPE at higher loadings. Our results from nanotube/semicrystalline polymer nanocomposites suggest that the interfacial thermal resistivity can be reduced by increasing the nucleation of crystallites at the SWNT/polymer interface.

Modeling Thermal Conductivity in Isotropic Composites. There are several methods to model the thermal conductivity of filled polymer composites. Guthy et al. fit thermal conductivity data of SWNT/amorphous polymer composites using the Nielson model, which assumes monodisperse rod-shaped fillers and perfect thermal conductivity between filler particles.[24,25] The thermal conductivity from this model critically depends on the SWNT aspect ratio. To obtain good agreement between the data and the Nielson model, Guthy et al. used a low thermal conductivity for the SWNT (~10 W/mK) that infers a high interfacial thermal resistance.

Nan et al. used effective medium theory (EMT) to describe the thermal conductivity enhancement observed in MWNT−oil suspensions, assuming that the MWNT are evenly coated with an oil layer.[26] The EMT specifically includes the effects of nanotube diameter *and* length (d, L), rather than their aspect ratio and has also been used to extract the interfacial thermal resistance, R_k, in SWNT/epoxy nanocomposites from experimentally determined thermal conductivities.[9] Applying this model to our SWNT/HDPE nanocomposite data with $\phi \leq 0.06$ SWNT, we use 3000 W/mK for the thermal conductivity of SWNT, an experimental value of 0.5 W/mK for the HDPE matrix, and 3 and 445 nm for the SWNT diameter d and length L, respectively.[16] The good fit of this model to our data at $\phi \leq 0.06$ (Figure 3) yields an interfacial thermal resistances, R_k, of $(1.0 \pm 0.3) \times 10^{-8}$ m^2 K/W, which is comparable to previous experimental and theoretical results.[9,11,27] This model provides a reasonable R_k, but as expected, it is not able to fit our data with $\phi \sim 0.2$ SWNT because the EMT model applies to composites in which the fillers are completely surrounded by the matrix.

Finally, we applied a nonlinear model presented by Foygel et al.[20] to our thermal conductivity data for SWNT/HDPE nanocomposites. This approach is based on percolating clusters (capped cylinders in a unit cube) and applies Monte Carlo simulations to develop key parameters (percolation threshold, conductivity exponent of percolation model, and contact resistance) for the electrical and thermal conductivity.[20] The conductivity of a nanotube composite in the vicinity of the percolation threshold is described by the following function:

$$\sigma(\phi;a) = \sigma_0[\phi - \phi_c(a)]^{t(a)} \quad (1)$$

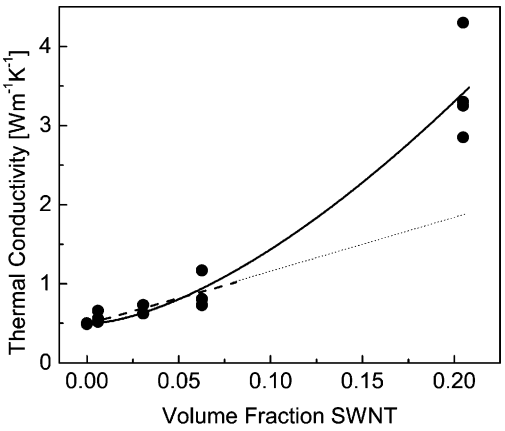

Figure 3. Thermal conductivity for isotropic (●) SWNT/HDPE nanocomposites at various SWNT volume fractions, where the thermal conductivities were measured perpendicular to the pressing direction. The effective medium theory was fit to $\phi \leq 0.06$ (dashed) and extended to higher ϕ (dotted). A percolation model was fit to $\phi \leq 0.20$ (solid).

where σ_0 is a preexponential factor that depends on the conductivity of the individual nanotubes and/or of the contacts between them as well as on the topology of the percolation cluster. ϕ is the volume fraction, ϕ_c is the critical volume fraction at the electrical percolation threshold, and $t(a)$ is a critical conductivity exponent for a given nanotube aspect ratio a. Using Foygel's results and the diameter and length of our SWNT bundles, we estimate $\phi_c = 0.003$. The least-square fit to eq 4 with σ_0 and $t(a)$ as fitting parameters provides $\sigma_0 = 36 \pm 5$ W/mK and $t(a) = 1.57 \pm 0.15$ for HDPE composites (Figure 3). The fit follows all of the experimental data points, suggesting that the thermal conductivity relies on a percolation SWNT network, rather than isolated nanofiller particles, even in the absence of a dramatic percolation threshold. The contact resistance R_0 is defined as

$$R_0 = (\sigma_0 L \phi_c^{t(a)})^{-1} \quad (2)$$

where L is the SWNT length. The obtained value for R_0, using the values for σ_0 and $t(a)$ obtained from the fit, is $(6 \pm 3) \times 10^8$ K/W. R_0 from this data analysis can be compared to R_k from EMT by assuming that 1/100 of each SWNT surface takes part in the heat conduction of the percolation network. Then the active interface per SWNT can be estimated as 4.2×10^{-17} m^2 (for SWNT diameter and length of 3 and 445 nm), from which the interfacial thermal resistance R_k is estimated as $(3 \pm 1.5) \times 10^{-8}$ m^2 K/W for $\phi_c \leq 0.20$ SWNT. This is the same order of magnitude as found with the effective medium theory for $\phi \leq 0.06$ SWNT. Thus, both models indicate an interfacial thermal resistance on the order of $(1-3) \times 10^{-8}$ m^2 K/W, where the EMT model is best applied to lower loadings ($\phi \leq 0.06$ SWNT in this case) and Foygel's percolation model is applicable to a wider range of loadings ($\phi \leq 0.20$ SWNT in this case). These findings suggest that while thermal conductivity of SWNT/polymer nanocomposites do not exhibit a dramatic increase at low loading, as widely observed in electrical conductivity, a percolation model might still be necessary to fit the thermal conductivity data at higher loadings.

Highly Aligned Composites. After probing the effect of crystallinity on the thermal conductivity in SWNT/PE nanocomposites and comparing to theoretical models, we now explore the influence of an aligned semicrystalline matrix and aligned SWNT on thermal conductivity. The thermal conductivities of various SWNT/HDPE nanocomposites are reported as a function of the Hermans orientation factor, f_c (Figure 4).

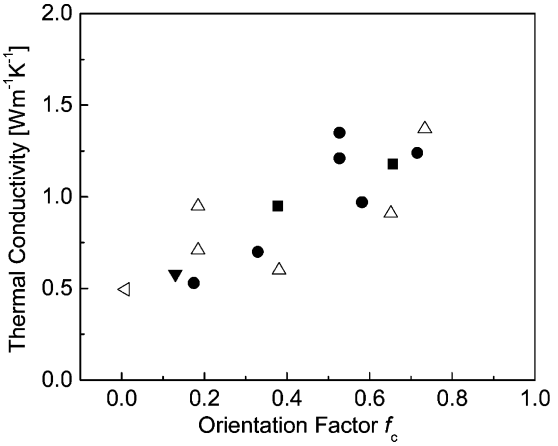

Figure 4. Thermal conductivity of various SWNT/HDPE nanocomposites as a function of the PE chain orientation, as given by f_c (see text for details): (tilted △) isotropic HDPE, (▼) nominally isotropic SWNT/HDPE with $\phi \sim 0.006$, (△) aligned HDPE fibers, (●) aligned SWNT/HDPE composites with $\phi \sim 0.006$, and (■) aligned SWNT/HDPE composites with $\phi \sim 0.012$. Thermal conductivities were measured along the alignment direction.

The orientation of HDPE in neat and composite samples was systematically varied from isotropic (recrystallized in a hot press) to highly aligned by using increasingly strong extensional flows (higher extrusion rates and higher wind-up speeds). Extensional flow aligns SWNT bundles, and given the tendency of SWNT to nucleate PE crystallization and to template PE lamellae growth perpendicular to the SWNT axis, both the matrix and filler are highly aligned after strong extensional flows. The Hermans orientation factor (f_c) describes the anisotropy of PE and increases from 0 to 1 with increasing alignment. Using wide-angle X-ray scattering, the angular orientation of a diffraction peak is used to calculate $f_c = (3\langle\cos^2\theta_c\rangle - 1)/2$, where θ_c is the angle between the fiber and the *c*-axis of orthorhombic PE crystal corresponding to the chain direction[28] (see ref 16 for details).

The thermal conductivity along the fiber direction increases with increasing f_c for both HDPE fibers and SWNT/HDPE composites. For example, the thermal conductivity increases by as much as 150% as f_c increases from 0 (isotropic) to ~0.65. Surprisingly, this increase is independent of SWNT loading ($\phi = 0$, 0.006, 0.012); there is no significant difference between HDPE and SWNT/HDPE composites. Therefore, the observed increase in thermal conductivity with increasing HDPE orientation for HDPE fibers and SWNT/HDPE composite fibers with low loadings is predominately caused by the alignment of the PE.

With respect to electrical conductivity, Du et al. have previously shown that SWNT alignment increases the loading necessary to form a SWNT network sufficient for electrical percolation.[29] Similarly, the electrical conductivity along the fiber direction of $\phi \sim 0.006$ and 0.012 SWNT/HDPE composite fibers with $f_c \sim 0.65$ is only $\sim 5 \times 10^{-10}$ S/cm, which is $\sim 10^6$ below the electrical conductivity of the corresponding isotropic sample.

Note that the SWNT loading is limited to $\phi \sim 0.012$ in Figure 4 because melt fiber spinning is not possible at higher loadings where the well-developed nanotube network impedes polymer motion. Our results suggest that alternative nanocomposite fabrication and processing methods that combine the effect aligning a semicrystalline matrix and higher SWNT loadings are likely to exhibit significantly higher thermal conductivities.

Conclusions

SWNT/PE composites made with HDPE (~78% crystalline) exhibit higher thermal conductivity than composites made with LDPE (~33% crystalline). Specifically, an isotropic SWNT/HDPE composite with $\phi \sim 0.2$ SWNT has a thermal conductivity twice as high as composites made with LDPE, reaching 3.5 W/mK. It appears that the higher crystallinity matrix reduces the interfacial thermal resistance by providing more crystalline-PE bridges between nanotubes. While the effective medium model adequately fits the thermal conductivity data at low loading in isotropic SWNT/HDPE nanocomposites, a percolation model was used to fit a wider range of filler compositions. Melt fiber spinning of SWNT/HDPE nanocomposites with low loadings produces composites in highly aligned SWNT and oriented polyethylene crystallites. The thermal conductivity along the alignment direction *increases* with PE alignment regardless of the SWNT loading, while the electrical conductivity along the fiber *decreases*. This study shows that the SWNT filler dominates the electrical conductivity of the SWNT/polymer composites, while the thermal conductivity depends comparably on both the SWNT filler and the semicrystalline PE matrix, thus suggesting new strategies for improving the thermal conductivity of SWNT/polymer nanocomposites.

Acknowledgment. Funding for this research was provided by the National Science Foundation (DMR-MRSEC 05-20020) and the Office of Naval Research (N00014-03-1-0890 and DURINT N00014-00-1-0720). We thank Dr. Leonard L. Yowell of NASA Johnson Space Center for supplying SWNT for this study.

References and Notes

(1) Berber, S.; Kwon, Y. K.; Tomanek, D. *Phys. Rev. Lett.* **2000**, *84*, 4613.
(2) Kim, P.; Shi, L.; Majumdar, A.; McEuen, P. L. *Phys. Rev. Lett.* **2001**, *87*, 215502.
(3) Yu, C.; Shi, L.; Yao, Z.; Li, D.; Majumdar, A. *Nano Lett.* **2005**, *5*, 1842.
(4) Pop, E.; Mann, D.; Wang, Q.; Goodson, K.; Dai, H. *Nano Lett.* **2006**, *6*, (1), 96.
(5) Biercuk, M. J.; Llaguno, M. C.; Radosavljevic, M.; Hyun, J. K.; Johnson, A. T.; Fischer, J. E. *Appl. Phys. Lett.* **2002**, *80*, 2767.
(6) Liu, C. H.; Huang, H.; Wu, Y.; Fan, S. S. *Appl. Phys. Lett.* **2004**, *84*, 4248.
(7) Choi, E. S.; Brooks, J. S.; Eaton, D. L.; Al-Haik, M. S.; Hussaini, M. Y.; Garmestani, H.; Li, D.; Dahmen, K. *J. Appl. Phys.* **2003**, *94*, 6034.
(8) Choi, S. U. S.; Zhang, Z. G.; Yu, W.; Lockwood, F. E.; Grulke, E. A. *Appl. Phys. Lett.* **2001**, *79*, 2252.
(9) Bryning, M. B.; Milkie, D. E.; Islam, M. F.; Kikkawa, J. M.; Yodh, A. G. *Appl. Phys. Lett.* **2005**, *87*, 161909.
(10) Moniruzzaman, M.; Winey, K. I. *Macromolecules* **2006**, *39*, 5194.
(11) Huxtable, S. T.; Cahill, D. G.; Shenogin, S.; Xue, L.; Ozisik, R.; Barone, P.; Usrey, M.; Strano, M. S.; Siddons, G.; Shim, M.; Keblinski, P. *Nat. Mater.* **2003**, *2*, 731.
(12) Shenogin, S.; Xue, L.; R. Ozisik; Keblinskia, P.; Cahill, D. G. *J. Appl. Phys.* **2004**, *95*, 8136.
(13) Choy, C. L. *Polymer* **1977**, *18*, 984.
(14) Choy, C. L.; Wong, Y. W.; Yang, G. W.; Kanamoto, T. *J. Polym. Sci., Part B: Polym. Phys.* **1999**, *37*, 3359.
(15) Hone, J.; Llaguno, M. C.; Nemes, N. M.; Johnson, A. T.; Fischer, J. E.; Walters, D. A.; Casavant, M. J.; Schmidt, J.; Smalley, R. E. *Appl. Phys. Lett.* **2000**, *77*, 666.
(16) Haggenmueller, R.; Fischer, J. E.; Winey, K. I. *Macromolecules* **2006**, *39*, 2964.
(17) Hone, J.; Whitney, M.; Piskoti, C.; Zettl, A. *Phys. Rev. B: Condens. Matter Mater. Phys.* **1999**, *59*, R2514.
(18) Benoit, J.-M.; Corraze, B.; Lefrant, S.; Blau, W.; Bernier, P.; Chauvet, O. *Synth. Met.* **2001**, *121*, 1215−1216.
(19) Du, F.; Scogna, R. C.; Zhou, W.; Brand, S.; Fischer, J. E.; Winey, K. I. *Macromolecules* **2004**, *37*, 9048.

(20) Foygel, M.; Morris, R. D.; Anez, D.; French, S.; Sobolev, V. L. *Phys. Rev. B: Condens. Matter Mater. Phys.* **2005**, *71*, 104201.
(21) Yu, A.; Itkis, M. E.; Bekyarova, E.; Haddon, R. C. *Appl. Phys. Lett.* **2006**, *89*, 133102.
(22) Shenogin, N.; Shenogin, S.; Xue, L.; Keblinski, P. *Appl. Phys. Lett.* **2005**, *87*, 133106.
(23) Krupa, I.; Novák, I.; Chodák, I. *Synth. Met.* **2004**, *145*, 245.
(24) Guthy, C.; Du, F.; Brand, S.; Fischer, J. E.; Winey, K. I. *MRS Proc. Fall Meeting* **2004**, HH (858E).
(25) Guthy, C.; Du, F.; Brand, S.; Winey, K. I.; Fischer, J. E., submitted to *J. Heat Transfer*.
(26) Nan, C. W.; Liu, G.; Lin, Y.; Li, M. *Appl. Phys. Lett.* **2004**, *85*, 3549.
(27) Maruyama, S.; Igarashi, Y.; Taniguchi, Y.; Shibuta, Y. *1st Int. Symp. Micro Nano Tech.* **2004**.
(28) Hermans, J. J.; Hermans, P. H.; Vermaas, D.; Weidinger, A. *Pays-Bas* **1946**, *65*, 427.
(29) Du, F.; Fischer, J. E.; Winey, K. I. *Phys. Rev. B: Condens. Matter Mater. Phys.* **2005**, *72*, 121404.

MA0615046